Structural Basis of Silencing: Sir3 BAH Domain in Complex with a Nucleosome at 3.0 Å Resolution
Karim-Jean Armache, *et al.*
Science **334**, 977 (2011);
DOI: 10.1126/science.1210915

This copy is for your personal, non-commercial use only.

If you wish to distribute this article to others, you can order high-quality copies for your colleagues, clients, or customers by clicking here.

Permission to republish or repurpose articles or portions of articles can be obtained by following the guidelines here.

The following resources related to this article are available online at www.sciencemag.org (this infomation is current as of January 11, 2012):

Updated information and services, including high-resolution figures, can be found in the online version of this article at:
http://www.sciencemag.org/content/334/6058/977.full.html

Supporting Online Material can be found at:
http://www.sciencemag.org/content/suppl/2011/11/17/334.6058.977.DC1.html

This article **cites 65 articles**, 33 of which can be accessed free:
http://www.sciencemag.org/content/334/6058/977.full.html#ref-list-1

This article appears in the following **subject collections:**
Biochemistry
http://www.sciencemag.org/cgi/collection/biochem

Downloaded from www.sciencemag.org on January 11, 2012

Science (print ISSN 0036-8075; online ISSN 1095-9203) is published weekly, except the last week in December, by the American Association for the Advancement of Science, 1200 New York Avenue NW, Washington, DC 20005. Copyright 2011 by the American Association for the Advancement of Science; all rights reserved. The title *Science* is a registered trademark of AAAS.

21. A. E. True, M. J. Nelson, R. A. Venters, W. H. Ormejohnson, B. M. Hoffman, *J. Am. Chem. Soc.* **110**, 1935 (1988).
22. S. J. Yoo, H. C. Angove, V. Papaefthymiou, B. K. Burgess, E. Munck, *J. Am. Chem. Soc.* **122**, 4926 (2000).
23. L. Noodleman, *J. Chem. Phys.* **74**, 5737 (1981).

Acknowledgments: S.D. thanks Cornell Univ. for financial support and the Alfred P. Sloan Foundation for a fellowship; F.N. acknowledges financial support from the Univ. of Bonn, the Max Planck Society, and the SFB 813; M.W.R. thanks the NIH for funding (grant R01-GM 67626). Portions of this research were carried out at the Stanford Synchrotron Radiation Lightsource (SSRL), a U.S. Department of Energy (DOE), Basic Energy Sciences user facility. The SSRL Structural Molecular Biology program is supported by DOE, Biological and Environmental Research, and NIH, National Center for Research Resources, Biomedical Technology Program.

Supporting Online Material
www.sciencemag.org/cgi/content/full/334/6058/974/DC1
SOM Text
Figs. S1 to S11
Tables S1 and S2
References (*24*–*35*)

1 April 2011; accepted 8 September 2011
10.1126/science.1206445

Structural Basis of Silencing: Sir3 BAH Domain in Complex with a Nucleosome at 3.0 Å Resolution

Karim-Jean Armache,[1,2] Joseph D. Garlick,[1,2] Daniele Canzio,[3,4] Geeta J. Narlikar,[3] Robert E. Kingston[1,2]*

Gene silencing is essential for regulating cell fate in eukaryotes. Altered chromatin architectures contribute to maintaining the silenced state in a variety of species. The silent information regulator (Sir) proteins regulate mating type in *Saccharomyces cerevisiae*. One of these proteins, Sir3, interacts directly with the nucleosome to help generate silenced domains. We determined the crystal structure of a complex of the yeast Sir3 BAH (bromo-associated homology) domain and the nucleosome core particle at 3.0 angstrom resolution. We see multiple molecular interactions between the protein surfaces of the nucleosome and the BAH domain that explain numerous genetic mutations. These interactions are accompanied by structural rearrangements in both the nucleosome and the BAH domain. The structure explains how covalent modifications on H4K16 and H3K79 regulate formation of a silencing complex that contains the nucleosome as a central component.

Eukaryotic cells normally carry the complete set of genes needed to specify every cell type. Establishment of a specific cell fate requires the silencing of genes whose expression would disrupt that fate. Several diverse families of protein complexes maintain silencing; however, the mechanisms involved are similar in *Saccharomyces cerevisiae* and in multicellular eukaryotes (*1*). Regulation of mating type loci in *S. cerevisiae* serves as a paradigm for silencing. Yeast growing as haploids can adopt two mating types, a and α. The genes that are expressed at the *MAT* loci determine cell fate, whereas genes specifying the opposite fate can be found at the silent *HMLα* or *HMRa* loci (*1*, *2*). The silent information regulator (Sir) proteins are essential for silencing of *HMLα* and *HMRa*, as well as telomeres and the ribosomal DNA (rDNA) loci (*1*, *2*).

The Sir proteins create domains of silenced chromatin. A long-standing hypothesis is that these proteins form specific repressive architectures that involve the basic unit of chromatin, the nucleosome. In support of this hypothesis, the SIR complex or Sir3 alone can compact nucleosomal arrays in vitro (*3*–*5*). The involvement of nucleosomes in the mechanism of silencing was first indicated by the observation that yeast could not silence *HMLα* and *HMRa* when they contained a mutated form of histone H4 with a deletion of the N-terminal tail (*6*). Subsequently, specific point mutations that affected silencing were found in the N-terminal tails and in the globular portions of core histones (*7*–*14*), and deacetylation of histone H4 was identified as a hallmark of silenced regions (*15*). Reporter gene expression, restriction enzyme accessibility, and micrococcal nuclease susceptibility were used to show that domains of silenced chromatin created by the SIR complex are several kb in length (*16*–*21*).

Several aspects of the extensive body of work on Sir3 interactions with nucleosomes are especially relevant to the structural work described here. Silencing requires deacetylation of histone H4 lysine 16 (H4K16); we describe the atomic contacts in the Sir3 binding pocket for H4K16. We also describe contacts with H3K79, whose methylation has the potential to modulate silencing. Many of the mutations in histones that affect silencing lie in the LRS (loss of rDNA silencing) (*11*, *12*) domain of the nucleosome core, and we describe numerous contacts between that region and Sir3. Mutations that affect silencing have been found both at the N terminus and at the C-terminal part of Sir3 (*22*). Most of these mutations are clustered in the bromo-associated homology (BAH) domain that is found in the N terminus of Sir3 (*23*–*26*). Here, we used a mutation in Sir3 (D205N) that confers increased binding to nucleosomes in vitro. Expression of the BAH D205N domain fused to LexA partially restores silencing of mating type loci in a *sir3* null background. This domain is able, therefore, to combine with Sir2 and Sir4 to cause partial silencing when it is attached to an ectopic dimerization domain (*27*).

We report the crystal structure of the complex of the hypermorphic D205N Sir3 BAH domain (BAH_{Sir3}) and the nucleosome core particle (NCP) at 3.0 Å resolution. Details of complex reconstitution, crystallization, data collection, and refinement can be found in the supporting online material (*28*). The BAH domain interacts extensively with each of the four core histones and, consequently, the solvent-accessible surface area buried between BAH_{Sir3} and the nucleosome is large (1750 $Å^2$, probe radius 1.4 Å). The structure shows a pseudo-two-fold symmetry, similar to that seen with the RCC1-nucleosome complex (*29*), in that BAH_{Sir3} interacts in a similar manner with each of the two opposite faces of the nucleosome (Fig. 1). We observed 30 residues of BAH_{Sir3} making contacts predominately with the core histones rather than nucleosomal DNA, suggesting that this protein-protein interface is critical to silencing.

Interactions with the core histones are mediated through five regions on the surface of BAH_{Sir3}. These regions map well to contacts inferred from genetic screens (see Figs. 1D and 2B for a summary). The BAH domain interacts with the H4 tail, which becomes folded upon binding, and the regions of histones H3 and H4 that make up the LRS domain. In addition, BAH_{Sir3} contacts histone H2B at a position adjacent to the LRS surface and the H2A/H2B acidic patch. Of the histone residues contacted by BAH_{Sir3} only one residue (H4V21) varies between the *Xenopus laevis* histones used here and yeast histones (Fig. 4B and fig. S3). Both of the histone residues that can be covalently modified and participate in the regulation of silencing (*7*–*9*, *30*) (H3K79 and H4K16) are ordered in the structure (Fig. 1B and below).

Interactions between BAH_{Sir3} and the nucleosome are established through flexible regions, which fold upon interaction (Fig. 2 and Fig. 1C). The structures of both the BAH domain and the NCP alone were determined previously (*27*, *31*, *32*), allowing comparison to the structure of the complex described here. One striking transition that accompanies assembly of the complex is folding and ordering of the histone H4 tail through extended interactions with loops 2 and 4 of BAH_{Sir3} (Fig.

[1]Department of Molecular Biology, Massachusetts General Hospital, Boston, MA 02114, USA. [2]Department of Genetics, Harvard Medical School, Boston, MA 02115, USA. [3]Department of Biochemistry and Biophysics, University of California, San Francisco, San Francisco, CA 94158, USA. [4]Chemistry and Chemical Biology Graduate Program, University of California, San Francisco, San Francisco, CA 94158, USA.

*To whom correspondence should be addressed. E-mail: kingston@molbio.mgh.harvard.edu

Downloaded from www.sciencemag.org on January 11, 2012

1C). Residues in flexible loops 1 and 3 of BAH_{Sir3} are completely disordered in a free BAH domain structure but become ordered and partially ordered, respectively, upon binding the core region of the nucleosome. Additionally, the N terminus of BAH_{Sir3}, which is in the vicinity of nucleosomal DNA (Fig. 1C), changes conformation upon binding the nucleosome. We conclude that BAH_{Sir3} forms contacts with a large area of the histone octamer and that regions of the nucleosome and BAH_{Sir3} become ordered upon this interaction.

Mutagenesis of the BAH domain of Sir3 has identified 40 amino acid residues that affect silencing (Fig. 2B) (*23*–*26*). BAH_{Sir3} contains at least 28 residues that form interactions (less than 4.1 Å distance) with a nucleosome. Of these, 17 were identified in genetic screens. Similarly, at least 30 mutations that affect silencing have been found in core histones (*6*, *10*–*14*, *23*, *25*, *33*, *34*), and the structure provides an atomic description for 14 of these residues (Fig. 1D; red depicts physical contacts; green, genetic contacts; yellow, overlap).

Many of these mutations map to complementary electrostatic interactions in the interface between histones and BAH_{Sir3}. In several instances, mutations that increase silencing increase the attractive charge in the interface between histones and the BAH domain, emphasizing the importance of this type of interaction to the creation of a silenced chromatin state. The extensive correlation between mutations and molecular contacts indicates that the crystal structure reflects contacts important to biological function. We present the details of these contacts, and how they might explain both the genetic analysis and the role for covalent modification of histones in silencing, by starting with the H4 tail region and then moving through the body of the nucleosome to the acidic patch in histone H2A and H2B.

The demonstration that the N terminus of histone H4 is critical for silencing in yeast was one of the initial findings indicating the importance of nucleosomes in transcriptional regulation. Deletions and mutations of the N terminus of H4 (4 to 29) relieve silencing at HMLα and HMRa but do not impact growth of yeast (*6*). The charge of H4 residues 16 to 19 (a basic patch) was shown to be essential for silencing because mutations that sustain the positive charge maintained repression, whereas mutations to glycine or glutamine abolished repression (*7*–*9*).

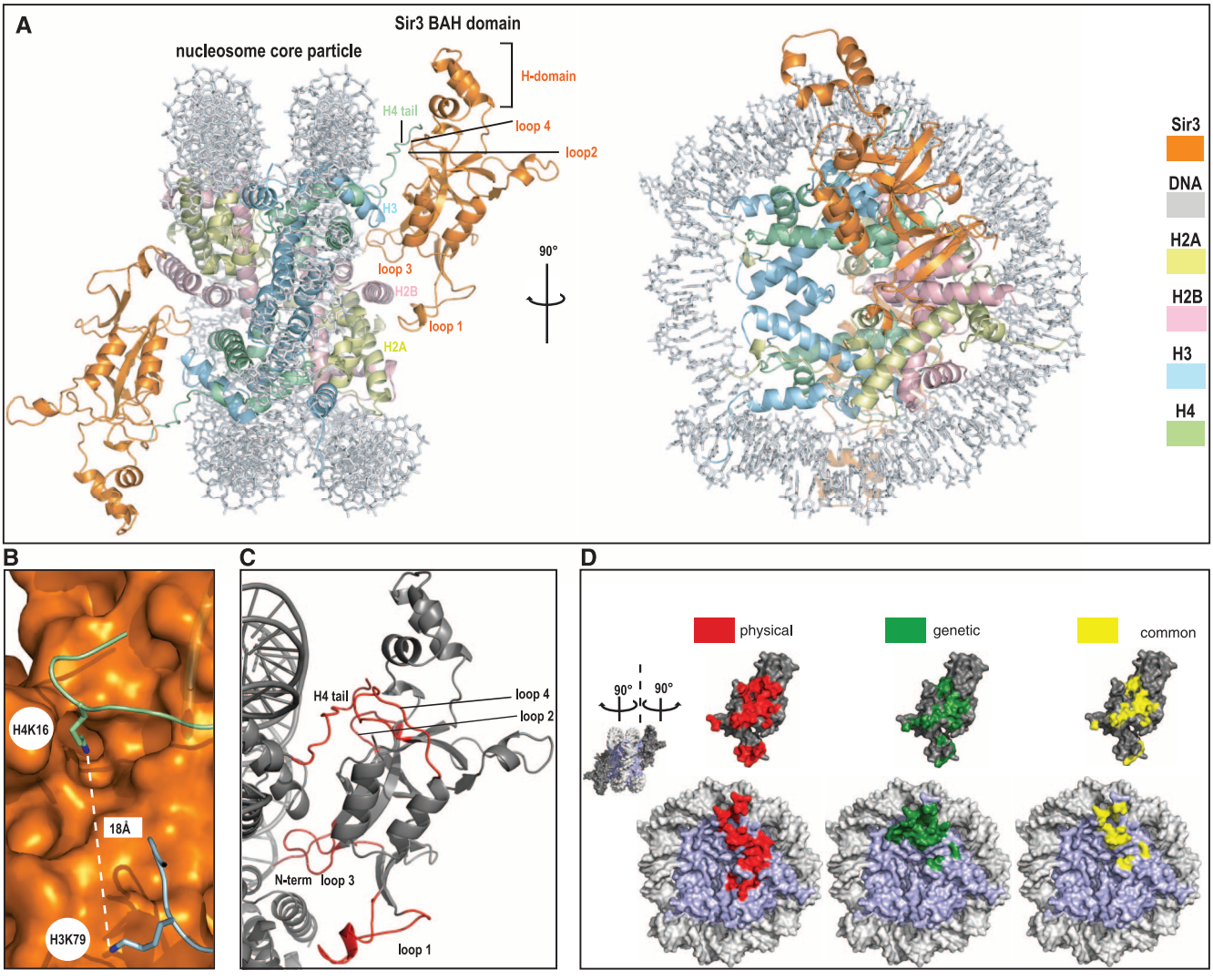

Fig. 1. (**A**) General overview of the structure. Two different views of the complex; front view and view rotated by 90° around the *y* axis. The structure is color coded (BAH domain is depicted in orange, H2A in yellow, H2B in light pink, H3 in blue, H4 in green, and DNA in light gray). (**B**) Histone H4K16 and histone H3K79. Both residues that are critical in the regulation of SIR complex mediated silencing are shown. Histone H4K16 is depicted in green, histone H3K79 in blue, and the BAH domain surface in orange. (**C**) Folding transitions in the complex. Both the nucleosome and the BAH domain are depicted in gray, and regions that get folded upon interaction are shown in red. (**D**) Correlation between structural and genetic contacts. Open-book view of the complex. The NCP surface is shown on the bottom and the BAH domain on top. Surfaces colored in red represent physical contacts as seen in the structure. Surfaces colored in green represent residues both in the NCP and the BAH domains where mutation has been shown to impact silencing. Yellow surfaces represent the overlay of physical (structure-derived) and genetic contacts.

Downloaded from www.sciencemag.org on January 11, 2012

The histone H4 tail becomes ordered through residue G13 due to stabilizing interactions with BAH_{Sir3}. The H4 tail region interacts with loops 2 and 4, strand B5, and helix A1 of BAH_{Sir3} (Fig. 3A). Each of these structural features contains residues whose mutation generates a silencing phenotype (Fig. 2). Additionally, one residue in BAH_{Sir3} located between strands B7 and B8 participates in this interaction (Fig. 3B). Binding interactions are largely electrostatic between the positively charged histone H4 tail and the negatively charged surface of the BAH domain (Fig. 3C). Sixteen residues in BAH_{Sir3} interact with H4 tail residues 13 to 23, primarily through their side chains (Fig. 3, B and C, and Fig. 4B) (*28*).

An essential role for H4K16 in silencing has been demonstrated by mutational analyses, by chromatin immunoprecipitation and coimmunoprecipitation studies, and by biochemical studies showing that acetylation of this residue disrupts Sir3 binding (*5*, *9*, *35*–*42*). A negatively charged binding pocket of BAH_{Sir3} accommodates the side chains of H4K16 and H4H18 (Fig. 3D). Specificity for H4K16 in the unmodified state is achieved primarily by hydrogen bonding and electrostatic interactions between the ε-amino group of H4K16 and several polar or negatively charged side chains of BAH_{Sir3} (Fig. 3E). Five of the BAH residues involved in contacts with K16 and H18 were identified in genetic screens. Of the potential electrostatic contacts that the BAH domain makes with histone residues 13 to 23 of the H4 N terminal tail, the majority are with K16 and H18. Acetylation of K16 could potentially disrupt most of the electrostatic contacts in this pocket (Fig. 3, D and E) and is therefore expected to decrease the affinity of Sir3 for the nucleosome, concordant with previous studies, which infer a 1000-fold impact of acetylation (*41*).

The LRS domain in the body of the nucleosome has been shown to be critically important for Sir3-dependent silencing at telomeres and at mating type loci (*11*, *12*). A systematic mutagenesis study demonstrated that residues 72 to 83 of histone H3 and 78 to 81 of histone H4 are important for silencing (*25*). The BAH domain makes extensive interactions with a surface of the nucleosome body that includes portions of histone H3, H4, and H2B and that extends from the base of the H4 tail to an H2A region (Fig. 2A). This surface is composed of helix α1 and loop L1 of histone H3, helix α2 and loop L2 of histone H4, and helices α3 and αC of histone H2B (Fig. 4A). The LRS interacting region of BAH_{Sir3} consists of loop 3, which becomes folded in the structure, as well as strands B6 and B8 and helix A8 (Fig. 4A). There are five LRS residues (Q76, D77, F78, K79, and T80) in helix α1 and loop L1 of H3 that contact loop 3 and strands B6 and B8 of BAH_{Sir3} (Fig. 4C). All five of these H3 residues were identified in the *slr* screen (*25*) (Fig. 4B). BAH residues contacting histone H3 are located on both the sides of loop 3 and in strands B6 and B8. Most of the residues in the BAH domain that interact with H3 in the LRS region have been identified as regulating silencing in genetic screens (Figs. 2B and 4C). Many additional contacts are seen between BAH_{Sir3} and other amino acids in the LRS (Fig. 4). The strong correlation between the genetics and the physical interactions support the importance of the contacts between the BAH domain and the LRS surface in generating silencing.

We were interested in understanding how the structural contacts made by D205N might lead to a hypermorphic phenotype. We see a potential hydrogen bond between the H3D77 side chain carbonyl and the BAH N205 side chain amide (Fig. 4C). In wild-type (WT) BAH_{Sir3}, the interaction between D205 and D77 would be a repulsive interaction, thereby explaining why the affinity of BAH_{Sir3} is increased by mutation to a neutral amino acid that can create hydrogen bonding in BAH D205N. Interestingly, mutations in H3D77 have also been shown to affect silencing (*25*). Mutations D77N and D77G would either increase binding to BAH D205 or remove repulsion, respectively, creating interactions similar to those seen in BAH D205N with the WT histone (Fig. 4C). Repulsive interactions have been proposed to limit binding affinity of WT Sir3 to the nucleosome, and this appears to be an important aspect of regulation. The BAH D205N mutation, which has increased binding affinity, causes increased telomeric silencing in some mutant backgrounds (*9*, *23*, *25*, *43*, *44*) but instead

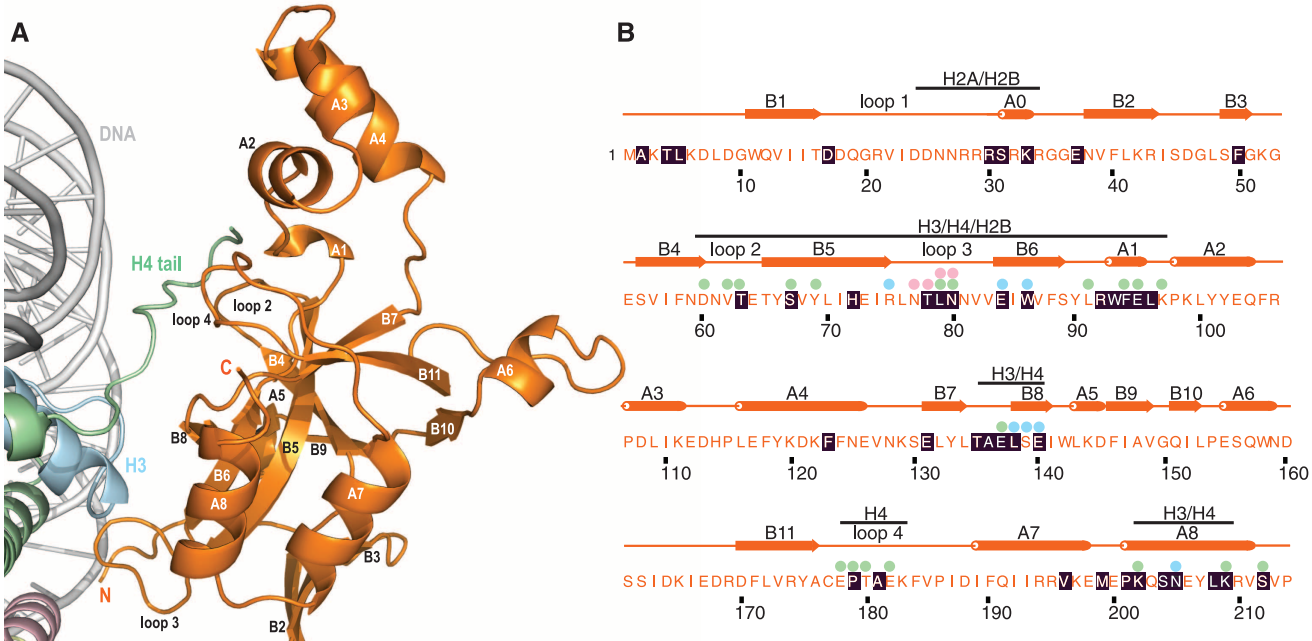

Fig. 2. Overview of interactions in the complex. (**A**) Same view as in Fig. 1A (front). BAH domain is depicted in orange, H2A in yellow, H2B in light pink, H3 in blue, H4 in green, and DNA in light gray. Secondary structure elements are also depicted here. Secondary structure was assigned using KSDSSP. (**B**) Primary and secondary structure of D205N BAH. Residues with black shading were mapped previously in genetic screens. Spheres above the sequence show histone interactions (within 4.1 Å) that are ordered and visible in the electron density. Colors of spheres represent which histone interacts with this residue of the BAH domain. Bars above the secondary structure indicate which histone is interacting with this particular region of the BAH domain. There are no spheres over the residues in loop1 (residues 17 to 37) because this region is poorly ordered.

Downloaded from www.sciencemag.org on January 11, 2012

causes decreased silencing in a WT background (*25*), perhaps due to increased affinity impairing function.

Methylation of H3K79 by Dot1p has been implicated in regulating silencing (*30*, *45*, *46*). This methylation event, which occurs in the LRS region of the body of the nucleosome, has been shown to decrease binding by Sir3 in vitro (*41*) and has been proposed to modulate silencing in vivo by preventing localization of Sir3 to non-silenced regions (*30*). H3K79 could potentially form three hydrogen bonds with BAH_{Sir3}, one to the side chain of E84 and two to the side chain of E140. H3K79 conformation is further stabilized by van der Waals interactions with BAH W86 and H4E74 (Fig. 4C). Methylation of H3K79 would increase the cationic radius and the hydrophobicity of this residue. Progressive methylation would decrease the potential of H3K79 to form hydrogen bonds, and trimethylation would ablate hydrogen bonding. This could potentially result in a decreased affinity of BAH_{Sir3} for the nucleosome.

It is remarkable that at least 16 H4 and H2B residues in the LRS and adjacent regions have the potential to interact with only five residues of BAH_{Sir3}. Mutation of four of these amino acids (T78, L79, N80, and K202) was shown to affect silencing in genetic screens, indicating the importance of this interface (Figs. 2B and 4D). In a manner similar to reciprocal mutations in BAH D205 and H3D77, the LRS mutations can be suppressed by a gain-of-function mutation BAH L79I, also identified in the *slr* screen. This mutation has the potential to increase van der Waals contacts with the BAH domain, elucidating a possible molecular mechanism for this genetic observation.

The acidic surface of histones H2A and H2B is a nucleosome interaction surface for proteins such as herpesvirus LANA (*47*) and RCC1 (*29*). A crystal-packing interaction between a basic region of histone H4 tail and the acidic patch on adjacent nucleosome is observed in the crystal lattice of the *Xenopus* NCP (*32*). The BAH domain apparently also makes contacts here, as evidenced by electron density adjacent to the acidic patch; this density is poor and not continuous, but can only be accounted for by residues 17 to 37 of BAH_{Sir3} (Fig. 4E). This region of the BAH domain is disordered in the apo structure (*27*). The density could be roughly modeled to locate the positively charged region of residues 28 to 34 of BAH_{Sir3} as being close to the acidic residues of H2A and H2B. Mutations of these residues in the BAH domain were shown to affect silencing (*24*, *25*). It is possible that in the context of the full protein, this interaction is stabilized and important for the overall affinity of Sir3 to nucleosome.

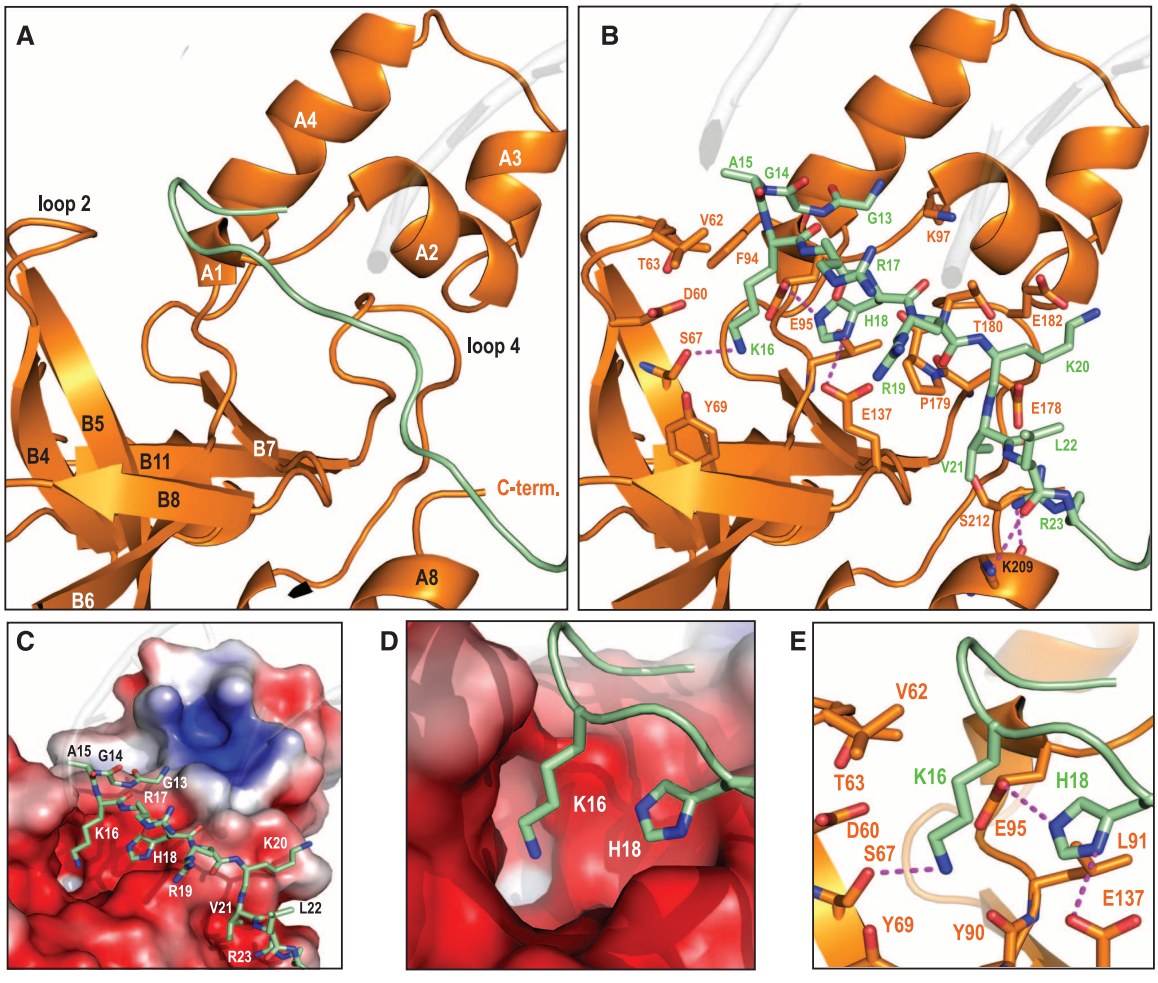

Fig. 3. Overview of H4 tail interactions. (**A**) General view of BAH structural elements that interact with histone H4. The BAH surface depicted here in orange interacts with the H4 tail in green. The interaction surface is in between two domains of BAH, the helical H domain and the β sheet, and loops 2 and 4 play a crucial role in this interaction. (**B**) Detailed view of the H4 tail interface. Same view as Fig. 3A. All H4 tail residues (13 to 23) are shown as sticks, whereas in BAH only residues that make contacts are depicted as sticks. Magenta dashes connect residues forming potential hydrogen bonds (≤3.5 Å). There are six possible hydrogen bonds in this interface; K16 forms one, H18 two, the R23 side chain two, and the L22 main chain carbonyl forms one. Other H4 residues that could participate in these polar interactions are K20 (with E182) and R23 (E178 HB and S212). G13, A15, V21, and R19 all make van der Waals interactions with numerous BAH residues (K97, F94, V62, T63, E95, L91, P179, T180, S212, and E178). Side-chain density for the majority of the H4 tail residues is visible (*28*), the exceptions being side chains of R17 and R19, which are apparently more flexible and display weak side-chain density. (**C**) Charge complementarity of the interface. Basic histone H4 tail interaction with a negatively charged BAH domain surface. APBS-calculated electrostatics (−5kT to 5kT). Red surface represents negative and blue positive charge, respectively. (**D**) Close-up view of H4K16 and H4H18 binding in the charged pocket. (**E**) K16 binding pocket in BAH. Detailed view of K16 and H18 side-chain interactions. The K16 ε-amino group interacts with polar or negatively charged side chains of the BAH domain (D60, Y69, E95, and S67). K16 appears to form a hydrogen bond with S67 (3.1 Å) and potentially a weak electrostatic interaction with the Y90 main chain carbonyl. Methyl groups of V62 and T63 could stabilize the alkyl chain of K16. Side-chain carbonyls of E137 and E95 and the main-chain carbonyl of P179 can form hydrogen bonds and an electrostatic interaction with the imidazole moiety of H18, respectively. H18 is additionally coordinated through van der Waals contacts.

Downloaded from www.sciencemag.org on January 11, 2012

How might the interface between the nucleosome and BAH_{Sir3} be integrated in a larger structure containing full-length Sir3 to compact long regions of chromatin? The Sir3 protein has features not studied here that contribute to silencing, including acetylation of the N terminus and dimerization determined by C- terminal regions (*22*, *48*–*51*). In addition, interactions involving other proteins, especially Sir4, might be important, although overexpression of Sir3 alone can increase the size of the silent domain, implicating Sir3 as a fundamental architectural protein in establishing these extended domains (*52*, *53*). To understand Sir3 oligomerization, we will need to determine structures of full-length Sir3 with nucleosome arrays. Even in light of these caveats, there are features of the crystal packing of the BAH_{Sir3}-NCP structure that suggest a possible contribution of the BAH domain to nucleosome compaction.

Adjacent nucleosomes in the crystal lattice are bridged by dimerization of the BAH domain (Fig. 4F and fig. S4). Interestingly, this dimer interface was also seen in the asymmetric unit of the apo BAH domain crystal lattice (*27*). To assess whether dimerization is solely a crystal-packing phenomenon, we used sedimentation velocity analytical ultracentrifugation to determine whether the BAH domain dimerizes in solution. Analysis of the weight-average sedimentation coefficient for the BAH domain shows the presence of a weak self-association process, with a dimerization constant of ~2 mM (fig. S5). This weak interaction is expected to be insufficient by itself to promote compacted structures, but might contribute in the context of the full-length Sir3 protein, which has additional self-association interfaces, and linked nucleosomes, which would increase the effective relative concentration of each half of this BAH homodimer interface.

The complex visualized here is anticipated to be one of the central components for establishment of the silent state of chromatin in yeast. The BAH domain of Sir3 binds to an extensive histone surface within the nucleosome, causing structural transitions in both BAH_{Sir3} and the H4 tail of the nucleosome. The correlation between mutations that affect silencing by Sir3 and amino acids that form physical contacts between BAH_{Sir3} and the nucleosome show that this structure is important in the generation of silencing. The importance of a broad contiguous face in the interaction is underscored by our finding that mutations initially isolated as suppressors of H4 tail mutations, such as D205N, enhance interactions in the body of the nucleosome that are physically distant from the tail interactions. Numerous previous

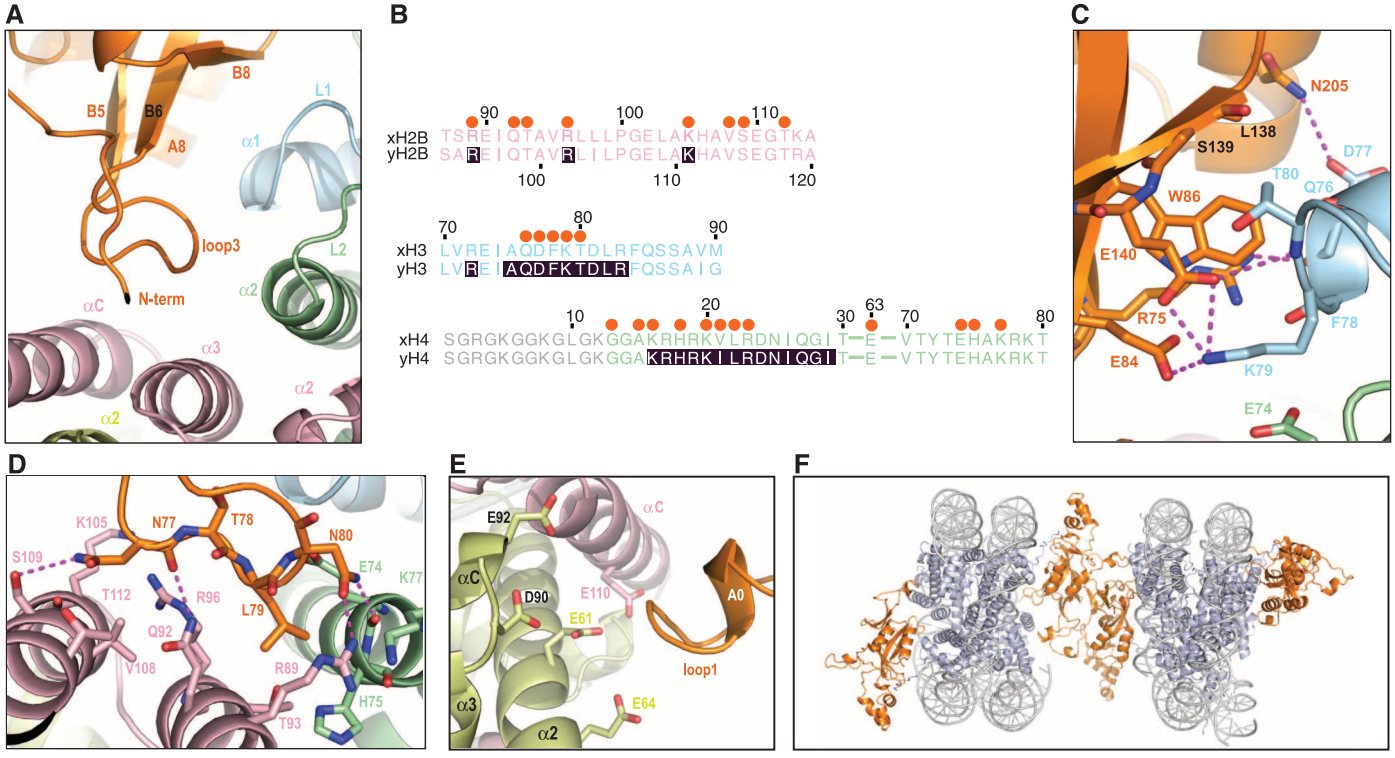

Fig. 4. Interactions of BAH domain with a NCP body. (**A**) General view of interactions in this region. Folded loop 3 and the β strands that interact with regions of histones H3, H4, and H2B are shown. (**B**) Sequence alignment of regions of *Xenopus* and yeast histones (color coded the same as structure) that interact with BAH domain. Shaded residues were described in previous genetic screens. Orange spheres above the sequence depict which residues interact with the BAH domain. The region of histone H4 that is disordered in the structure is depicted in gray. (**C**) Detailed interactions of BAH with H3. A magnified view of the top part of (A). Magenta dashes connect residues forming potential hydrogen bonds. Five LRS (Q76, D77, F78, K79, and T80) residues in helix α1 and loop L1 of H3 that contact the BAH domain in the structure. BAH W86 is within 4 Å of the H3Q76 carbonyl, T80 side chain, and K79 Cα. There is a potential hydrogen bond between the H3D77 side-chain carbonyl and the BAH N205 side-chain amide. K79 could potentially form three hydrogen bonds with the BAH domain, one to the side chain of E84 and two to the E140 side chain. K79 conformation is further stabilized by van der Waals interactions with BAH W86 and H4E74. The T80 side chain interacts with the main chain of L138 and S139. BAH R75 forms polar interactions, one of which is a potential hydrogen bond with the main chain of H3 residues D77 and F78. Additionally, a hydrogen bond might also be formed between the BAH E140 side-chain carbonyl and the main-chain amide of H3 T80. (**D**) Detailed interactions of BAH with H4 and H2B. A magnified view of the bottom part of (A). Magenta dashes connect residues forming potential hydrogen bonds. Two residues at the tip of loop 3 (L79 and N80) interact with histones H4 and histone H2B. They make van der Waals contacts with histone H4 residues E74, H75, and K77. Additionally, the BAH N80 side chain could form hydrogen bonds with main-chain carbonyl of H4E74 and side chain of H2B R89. L79 interacts with three H2B residues in helix a3 (R89, T93, and Q92). BAH N77 and T78 main-chain carbonyls make charged interactions and a potential hydrogen bond with side chains of H2B residues R96 and Q92, respectively. The side chain of BAH N77 can additionally interact with four residues of H2B located in helix αC. (**E**) Interaction of the BAH domain with the acidic patch, same view as in Fig. 1 (front). A positively charged BAH patch (residues 28 to 34) is in close proximity to acidic residues E61, E64, D90, and E92 of H2A as well as residue E110 of H2B. (**F**) Crystal packing interaction.

Downloaded from www.sciencemag.org on January 11, 2012

studies have implicated nucleosomes as being important for regulation through either their physical location on the genome relative to regulatory sites or their covalent modification to specify docking of regulatory complexes. We extend these examples by describing an extensive interface between a regulatory factor and the core histones of the nucleosome, thereby showing how the nucleosome can be a direct component of regulation.

It is instructive to note how covalent modification of histones affects formation of this complex. Both acetylation of H4K16 and methylation of H3K79 are expected to disrupt several interactions that contribute to the BAH_{Sir3}-NCP interface. Acetylation of K16 is the more important of these modifications in vivo and would disrupt a larger number of molecular interactions based on the structure. Thus, with this complex, covalent modification of histones does not create a docking interface but rather has the potential to disrupt contacts and thereby cause a substantial change in the energetics of interaction.

References and Notes

1. L. N. Rusche, A. L. Kirchmaier, J. Rine, *Annu. Rev. Biochem.* **72**, 481 (2003).
2. S. Loo, J. Rine, *Annu. Rev. Cell Dev. Biol.* **11**, 519 (1995).
3. S. J. McBryant, C. Krause, C. L. Woodcock, J. C. Hansen, *Mol. Cell. Biol.* **28**, 3563 (2008).
4. F. Martino *et al.*, *Mol. Cell* **33**, 323 (2009).
5. A. Johnson *et al.*, *Mol. Cell* **35**, 769 (2009).
6. P. S. Kayne *et al.*, *Cell* **55**, 27 (1988).
7. P. C. Megee, B. A. Morgan, B. A. Mittman, M. M. Smith, *Science* **247**, 841 (1990).
8. E. C. Park, J. W. Szostak, *Mol. Cell. Biol.* **10**, 4932 (1990).
9. L. M. Johnson, P. S. Kayne, E. S. Kahn, M. Grunstein, *Proc. Natl. Acad. Sci. U.S.A.* **87**, 6286 (1990).
10. L. M. Johnson, G. Fisher-Adams, M. Grunstein, *EMBO J.* **11**, 2201 (1992).
11. J. H. Park, M. S. Cosgrove, E. Youngman, C. Wolberger, J. D. Boeke, *Nat. Genet.* **32**, 273 (2002).
12. J. S. Thompson, M. L. Snow, S. Giles, L. E. McPherson, M. Grunstein, *Genetics* **163**, 447 (2003).
13. M. N. Kyriss, Y. Jin, I. J. Gallegos, J. A. Sanford, J. J. Wyrick, *Mol. Cell. Biol.* **30**, 3503 (2010).
14. J. Dai, E. M. Hyland, A. Norris, J. D. Boeke, *Genetics* **186**, 813 (2010).
15. M. Braunstein, R. E. Sobel, C. D. Allis, B. M. Turner, J. R. Broach, *Mol. Cell. Biol.* **16**, 4349 (1996).
16. D. J. Mahoney, J. R. Broach, *Mol. Cell. Biol.* **9**, 4621 (1989).
17. S. Loo, J. Rine, *Science* **264**, 1768 (1994).
18. R. Schnell, J. Rine, *Mol. Cell. Biol.* **6**, 494 (1986).
19. L. Sussel, D. Shore, *Proc. Natl. Acad. Sci. U.S.A.* **88**, 7749 (1991).
20. K. A. Nasmyth, *Cell* **30**, 567 (1982).
21. D. E. Gottschling, O. M. Aparicio, B. L. Billington, V. A. Zakian, *Cell* **63**, 751 (1990).
22. S. Ehrentraut *et al.*, *Genes Dev.* **25**, 1835 (2011).
23. V. Sampath *et al.*, *Mol. Cell. Biol.* **29**, 2532 (2009).
24. E. M. Stone, C. Reifsnyder, M. McVey, B. Gazo, L. Pillus, *Genetics* **155**, 509 (2000).
25. A. Norris, M. A. Bianchet, J. D. Boeke, *PLoS Genet.* **4**, e1000301 (2008).
26. J. R. Buchberger *et al.*, *Mol. Cell. Biol.* **28**, 6903 (2008).
27. J. J. Connelly *et al.*, *Mol. Cell. Biol.* **26**, 3256 (2006).
28. Materials and methods are available as supporting material on *Science* Online.
29. R. D. Makde, J. R. England, H. P. Yennawar, S. Tan, *Nature* **467**, 562 (2010).
30. F. van Leeuwen, P. R. Gafken, D. E. Gottschling, *Cell* **109**, 745 (2002).
31. Z. Hou, J. R. Danzer, C. A. Fox, J. L. Keck, *Protein Sci.* **15**, 1182 (2006).
32. K. Luger, A. W. Mäder, R. K. Richmond, D. F. Sargent, T. J. Richmond, *Nature* **389**, 251 (1997).
33. Q. Yu, L. Olsen, X. Zhang, J. D. Boeke, X. Bi, *Genetics* **188**, 291 (2011).
34. C. J. Fry, A. Norris, M. Cosgrove, J. D. Boeke, C. L. Peterson, *Mol. Cell. Biol.* **26**, 9045 (2006).
35. O. M. Aparicio, B. L. Billington, D. E. Gottschling, *Cell* **66**, 1279 (1991).
36. M. Oppikofer *et al.*, *EMBO J.* **30**, 2610 (2011).
37. G. J. Hoppe *et al.*, *Mol. Cell. Biol.* **22**, 4167 (2002).
38. K. Luo, M. A. Vega-Palas, M. Grunstein, *Genes Dev.* **16**, 1528 (2002).
39. L. N. Rusché, A. L. Kirchmaier, J. Rine, *Mol. Biol. Cell* **13**, 2207 (2002).
40. J. C. Tanny, D. S. Kirkpatrick, S. A. Gerber, S. P. Gygi, D. Moazed, *Mol. Cell. Biol.* **24**, 6931 (2004).
41. M. Onishi, G. G. Liou, J. R. Buchberger, T. Walz, D. Moazed, *Mol. Cell* **28**, 1015 (2007).
42. A. Hecht, T. Laroche, S. Strahl-Bolsinger, S. M. Gasser, M. Grunstein, *Cell* **80**, 583 (1995).
43. Y. Park, J. Hanish, A. J. Lustig, *Genetics* **150**, 977 (1998).
44. C. Liu, A. J. Lustig, *Genetics* **143**, 81 (1996).
45. M. S. Singer *et al.*, *Genetics* **150**, 613 (1998).
46. H. H. Ng, D. N. Ciccone, K. B. Morshead, M. A. Oettinger, K. Struhl, *Proc. Natl. Acad. Sci. U.S.A.* **100**, 1820 (2003).
47. A. J. Barbera *et al.*, *Science* **311**, 856 (2006).
48. H. Liaw, A. J. Lustig, *Mol. Cell. Biol.* **26**, 7616 (2006).
49. G. G. Liou, J. C. Tanny, R. G. Kruger, T. Walz, D. Moazed, *Cell* **121**, 515 (2005).
50. D. A. King *et al.*, *J. Biol. Chem.* **281**, 20107 (2006).
51. S. J. McBryant, C. Krause, J. C. Hansen, *Biochemistry* **45**, 15941 (2006).
52. H. Renauld *et al.*, *Genes Dev.* **7**, (7A), 1133 (1993).
53. A. Hecht, S. Strahl-Bolsinger, M. Grunstein, *Nature* **383**, 92 (1996).

Acknowledgments: This work was supported by grant GM043901 from NIH (to R.E.K.). K-J.A. was supported in part by a fellowship from the Human Frontier Science Program. We thank the staff at Beamlines 24-IDC/E at Argonne National Laboratory, especially K. Rajashankar and F. Murphy, for excellent assistance with data collection. We thank R. Sternglanz for BAH domain constructs. We thank T. Schwartz for use of the high-throughput crystallization facility, as well as helpful discussions and critical reading of the manuscript. We thank F. Winston for critical reading of the manuscript. We thank S. Jenni and D. Kostrewa for helpful discussions; S. Tan and K. Luger for help with technical aspects of forming nucleosomes; J. Cochrane, S. Bowman, S. Miller, M. Simon, and K. Bouazoune for critical reading of the manuscript, and members of the Kingston laboratory for helpful discussions. Coordinates and structure factors have been deposited in the Protein Data Bank with accession code 3TU4.

Supporting Online Material

www.sciencemag.org/cgi/content/full/334/6058/977/DC1
Materials and Methods
SOM Text
Figs. S1 to S5
Table S1
References (*54*–*68*)

8 July 2011; accepted 29 September 2011
10.1126/science.1210915

Active Starvation Responses Mediate Antibiotic Tolerance in Biofilms and Nutrient-Limited Bacteria

Dao Nguyen,[1]† Amruta Joshi-Datar,[2] Francois Lepine,[3] Elizabeth Bauerle,[2] Oyebode Olakanmi,[4] Karlyn Beer,[2] Geoffrey McKay,[1] Richard Siehnel,[2] James Schafhauser,[1] Yun Wang,[5] Bradley E. Britigan,[4,6]* Pradeep K. Singh[2]

Bacteria become highly tolerant to antibiotics when nutrients are limited. The inactivity of antibiotic targets caused by starvation-induced growth arrest is thought to be a key mechanism producing tolerance. Here we show that the antibiotic tolerance of nutrient-limited and biofilm *Pseudomonas aeruginosa* is mediated by active responses to starvation, rather than by the passive effects of growth arrest. The protective mechanism is controlled by the starvation-signaling stringent response (SR), and our experiments link SR-mediated tolerance to reduced levels of oxidant stress in bacterial cells. Furthermore, inactivating this protective mechanism sensitized biofilms by several orders of magnitude to four different classes of antibiotics and markedly enhanced the efficacy of antibiotic treatment in experimental infections.

In the laboratory, marked antibiotic tolerance can be produced by starving bacteria for nutrients (*1*). Starvation also contributes to tolerance during infection, as nutrients become limited when they are sequestered by host defenses and consumed by proliferating bacteria (*2*, *3*). One of the most important causes of starvation-induced tolerance in vivo is biofilm growth, which occurs in many chronic infections (*4*–*6*). Starvation in biofilms is due to nutrient consumption by cells located on the periphery of biofilm clusters and by reduced diffusion of substrates through the biofilm (*7*). Biofilm bacteria show extreme tolerance to almost all antibiotic classes, and supplying limiting substrates can restore sensitivity (*8*).

[1]Departments of Medicine, Microbiology and Immunology, McGill University, 1650 Cedar Avenue, L11.513, Montreal, Quebec H3G 1A4, Canada. [2]Departments of Medicine and Microbiology, University of Washington School of Medicine, 1959 Northeast Pacific Street, Seattle, WA 98195–7242, USA. [3]Department of Microbiology, INRS Armand Frappier, 531 Boulevarde des Prairies, Laval, Quebec H7V 1B7, Canada. [4]Department of Internal Medicine, University of Cincinnati, Medical Sciences Building 6065, Post Office Box 670557, Cincinnati, OH 45267, USA. [5]Department of Civil and Environmental Engineering, Northwestern University, A222 Technological Institute, 2145 Sheridan Road, Evanston, IL 60208, USA. [6]Veterans Administration Medical Center–Cincinnati, 3200 Vine Street, Cincinnati, OH 45220, USA.

*Present address: College of Medicine, University of Nebraska, 42nd and Emile, Omaha, NE 68198, USA.
†To whom correspondence should be addressed. E-mail: dao.nguyen@mcgill.ca

Downloaded from www.sciencemag.org on January 11, 2012